

FEBRUARY 02 2011

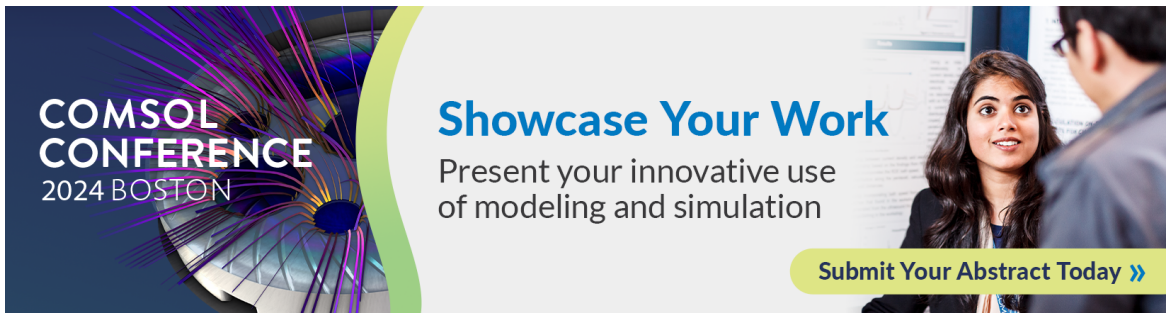
# The effect of coupling on bubble fragmentation acoustics

Helen Czerski; Grant B. Deane



*J. Acoust. Soc. Am.* 129, 74–84 (2011)

<https://doi.org/10.1121/1.3514416>



**COMSOL CONFERENCE**  
2024 BOSTON

## Showcase Your Work

Present your innovative use of modeling and simulation

[Submit Your Abstract Today >>](#)

# The effect of coupling on bubble fragmentation acoustics

Helen Czerski<sup>a)</sup> and Grant B. Deane

*Marine Physical Laboratory, Scripps Institution of Oceanography, La Jolla, California 92093-0238*

(Received 6 October 2009; revised 6 July 2010; accepted 7 October 2010)

Understanding the formation and evolution of bubble populations is important in a wide range of situations, including industrial processes, medical applications, and ocean science. Passive acoustical techniques can be used to track changes in the population, since each bubble formation or fragmentation event is likely to produce sound. This sound potentially contains a wealth of information about the fragmentation process and the products, but to fully exploit these data it is necessary to understand the physical processes that determine its characteristics. The focus of this paper is binary fragmentation, when turbulence causes one bubble to split into two. Specifically, the effect that bubble-bubble coupling has on the sound produced is examined. A numerical simulation of the acoustical excitation of fragmenting bubbles is used to generate model acoustic signals, which are compared with experimental data. A frequency range with a suppressed acoustic output which is observed in the experimental data can be explained when coupling is taken into account. In addition, although the driving mechanism of neck collapse is always consistent with the data for the larger bubble of the newly formed pair, a different mechanism must be driving the smaller bubble in some situations.

© 2011 Acoustical Society of America. [DOI: 10.1121/1.3514416]

PACS number(s): 43.30.Nb [KGF]

Pages: 74–84

## I. INTRODUCTION

Relatively little is known about the evolving bubble populations in the first second after a wave breaks, due to the difficulty of making direct measurements. Highly turbulent conditions cause large bubbles to fragment repeatedly, until they are small enough for surface tension to stabilize them by preventing significant distortion. Soon after this, the largest bubbles will rise to the surface and be lost from the population. It has been shown that bubbles from breaking waves,<sup>1</sup> and particularly the brief existence of larger bubbles,<sup>2,3</sup> has significant consequences for air-sea gas exchange, and so accurate measurements of the evolving bubble population are highly desirable.

The evolution of bubble clouds in turbulence is a complex process, and several methods have been used to follow the rapidly changing bubble population. Optical data<sup>4</sup> are difficult to acquire and require very careful analysis but are capable of measuring very early bubble populations directly. Active acoustic methods can be very effective at inferring the bubble population by measuring its effect on the bulk acoustic properties of the water.<sup>5,6</sup> However, in the first second after a wave breaks, very high air fraction will cause signal attenuation in excess of 100 dB/m, which is too much for a useful measurement. Passive acoustic techniques have also been used when individual bubble pulses can be identified,<sup>7–9</sup> and these interpret the sounds produced naturally by the evolving cloud to infer the bubble population within. Passive acoustic methods have the advantage of being remote and therefore non-intrusive. Improving these methods is the aim of the research presented in this paper. It is well-known that a newly formed bubble oscillates at its natural frequency

(which is determined largely by the bubble radius) and so the frequency of the acoustic emission has commonly been used as a proxy for the bubble size.<sup>8,10,11</sup> This approach suffices for a quick and simple measurement, but it ignores the physics of the fragmentation processes by which new bubbles are formed in turbulent conditions. A better knowledge of this physics and the associated mechanisms of sound production could improve interpretation of passive acoustic data significantly.

Many researchers have considered the sounds produced by bubble rescaling,<sup>12–14</sup> but almost all of them studied a spherical bubble driven by an external periodic pressure oscillation. In nature, oscillations are also likely to be excited by a single impulsive event associated with bubble formation. Several authors<sup>15–19</sup> have speculated on the mechanisms which link the bubble formation event to the sound-producing volume oscillation. Suggestions have included an internal pressure increase associated with the Laplace pressure, hydrostatic pressure effects, and shape mode coupling. Most recently, Deane and Czerski<sup>20</sup> showed that the sound produced by a bubble formed at a nozzle was consistent with the forcing caused by the rapid collapse of the neck of air left after bubble pinch-off. This mechanism could also be active when one bubble splits into two during turbulent distortion, and long necks have been observed at the moment of fragmentation.<sup>21</sup> In the same paper, it was shown that for symmetrical fragmentation events, this mechanism produces amplitudes similar to those seen in fragmentation experiments.

The aim of this paper is to examine the effects of bubble-bubble coupling on the sound produced by a binary fragmentation event. The two new oscillators are very close, and the sound radiated by each one would be expected to influence the other.<sup>22,23</sup> The approach here is to use the neck-collapse mechanism to drive two axisymmetric bubbles, simulating two bubbles just after binary fragmentation. By numerically solving the equations describing the bubble dynamics for the two

<sup>a)</sup> Author to whom correspondence should be addressed. Current address: Graduate School of Oceanography, University of Rhode Island, South Ferry Road, Narragansett, RI 02882. Electronic mail: H.Czerski.97@cantab.net

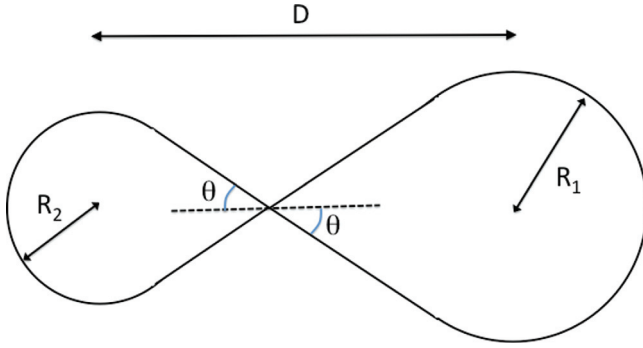


FIG. 1. (Color online) The bubble configuration assumed in this model at the point of pinch-off ( $t = 0$ ). The bubbles have cylindrical symmetry about their long axis, and each bubble is assumed to have the same conical neck angle  $\theta$ .  $R_1$  is always the radii of the larger bubble.

coupled bubbles, we can assess the effects of this coupling and explore its influence on future analysis of passive acoustic signals.

## II. MODEL

The numerical simulations done were straightforward, but it is important to discuss some of the details and assumptions involved. The model is summarized here to provide a context for the details which follow. Before each individual simulation, the radii of the two new bubbles were specified. The simulation starts at the moment of separation (pinch-off), when the two bubbles are assumed to have conical necks which almost touch at the apex, and the system has cylindrical symmetry. Figure 1 shows the initial bubble shape and the chosen parameters. As the simulation proceeds, each neck collapses inward toward the bubble center because of the newly unbalanced surface tension forces. This rapidly reduces the volume of each individual bubble and therefore stimulates sound-producing volume oscillations.<sup>20</sup> Each bubble response is calculated using the Rayleigh-Plesset equation, and the acoustic signal produced by each bubble is calculated from its surface acceleration [Ref. 13, Eq. (3.128)]. For each simulation, the user chooses whether to include non-linear terms in the Rayleigh-Plesset equation and whether the bubbles are coupled. At the end of the simulation, the superposed pressure pulses from the two bubbles are calculated at one meter from the rupture point and these are treated as simulated data to be compared with the superposed pulses measured in a fragmentation experiment. The total model coupled and uncoupled pulses are fitted with two decaying sinusoids, which were then compared with the individual pulse components from each bubble in the pair in order to assess the effect of the non-linear terms and bubble-bubble coupling.

### A. Details of the model calculations

The coupled Rayleigh-Plesset equations used here are set out below.<sup>24</sup> The bubbles are labeled 1 and 2, with equilibrium radii  $R_1$  and  $R_2$ .

$$\begin{aligned} \frac{d^2 r_1}{dt^2} = & \frac{-3L}{2} \left( \frac{dr_1}{dt} \right)^2 - \frac{3\kappa r_1 P_0}{\rho R_1^2} - 0.0025 \left( \frac{\omega_1}{2\pi} \right)^{1/3} \omega_1 \frac{dr_1}{dt} \\ & - N(R_1, \theta, t) - K \frac{R_2^3}{DR_1^2} \frac{d^2 r_2}{dt^2} \end{aligned} \quad (1)$$

$$\begin{aligned} \frac{d^2 r_2}{dt^2} = & \frac{-3L}{2} \left( \frac{dr_2}{dt} \right)^2 - \frac{3\kappa r_2 P_0}{\rho R_2^2} - 0.0025 \left( \frac{\omega_2}{2\pi} \right)^{1/3} \omega_2 \frac{dr_2}{dt} \\ & - N(R_2, \theta, t) - K \frac{R_1^3}{DR_2^2} \frac{d^2 r_1}{dt^2}, \end{aligned} \quad (2)$$

where  $r_{1,2}$  are the radii of bubbles 1 and 2 (not the fractional change in radius, as is used by some authors),  $t$  is time,  $L$  is 0 or 1 depending on whether the non-linear term in the Rayleigh-Plesset equation is being included or not,  $N(R_1, \theta t)$  is the forcing on bubble 1 from its own conical neck (discussed below) and the final term represents the pressure forcing on bubble 1 from bubble 2 or vice versa.  $K$  is 0 or 1 depending on whether the bubbles are to be coupled or not.  $P_0$  is the hydrostatic pressure in the water surrounding the bubbles,  $\kappa$  is the polytropic index (assumed to be 1.4 throughout),  $\rho$  is the density of water,  $D$  is the separation of the bubble centers (discussed below),  $\theta$  is the semi-angle of the conical neck (which is the same for both bubbles) and  $\omega_{1,2}$  is the natural frequency of the bubble.

The third term on the right-hand side of Eqs. (1) and (2) accounts for damping of the bubble breathing mode oscillations through radiation losses and thermal effects. The term used is an approximation following that in Medwin<sup>25</sup> for the damping of a bubble at its natural frequency. For larger bubbles like the ones considered here, radiation and thermal damping are expected to be significantly more important than viscous damping. A complete calculation would allow the damping to vary with the driving frequency, as set out by Prosperetti,<sup>12,26</sup> but these full calculations are far more computationally expensive and would only change the value slightly in this case. An important point to note is that the damping terms in the Rayleigh-Plesset equation are derived in frequency space for a steady driving force and a continuous response.<sup>12</sup> The driving term here (the neck collapse) is not periodic, but we assume that a result correct to first order may be obtained by simply adding in the non-periodic forcing in place of a periodic forcing function. This approach produced reasonable results in Deane and Czerski.<sup>20</sup>

The Rayleigh-Plesset equations for each bubble are simultaneously numerically integrated with respect to time using fourth order Runge-Kutta integration. Each simulation starts at the point where the bubbles have just separated and runs for 20 ms. This allows time for at least 30 oscillations for the larger bubble and more for the smaller bubble, which is more than adequate to fit the signals.

### B. Forcing terms

The rapid volume decrease resulting from the neck collapse is caused by the dynamics of the surface, not by the gas inside or the water outside the bubble. The inward acceleration of the bubble wall caused by the small radius of curvature results in a rapid bubble volume decrease as the neck collapses, so that a rarefaction propagates outward into the liquid. For a short period just after pinch-off, the bubble wall displacement, velocity, and acceleration are all simultaneously directed inward, and it is this unusual situation that leads to the rarefaction. The bubble is then assumed to respond to the rapid volume forcing according to the Rayleigh-Plesset equation, and

the volume forcing is assumed to be spherically symmetric. The subtleties of this mechanism are discussed in more detail in Deane and Czerski.<sup>20</sup>

Previous research<sup>20,21</sup> has suggested that the forcing  $f$  from the conical neck for a bubble with radius  $R = 2$  mm slowly released from a nozzle can be approximated by

$$f(\theta, t) = \frac{9\kappa\sigma P_o \tan^2 \theta}{4\rho^2 R^5 \sin \theta} t^{469.5t+1.955}. \quad (3)$$

This equation resulted from a study of one bubble size only, and for the model described here we need to model bubbles with a range of radii. Bubbles of different sizes would not be expected to have the same forcing with time, so it was necessary to estimate the change in the time-dependence of the forcing term with radius. Close to the start of the cone collapse, we expect the form of the forcing term to remain unchanged, since it seems reasonable that the shape and size of the rest of the bubble has little effect at very early times. We assume that the collapse is entirely driven by surface tension, dependent only on the cone angle, but after some time other factors will limit this collapse. To estimate this effect we chose to use a “window” function to adjust the driving force in a qualitatively reasonable way for different bubble radii. The neck-collapse forcing shown in Eq. (3) decays with time because the rest of the bubble starts to influence the dynamics of the collapse. We expect that this forcing will decay more quickly for smaller bubbles because the rest of the bubble will influence the dynamics after a shorter time. Consequently, we chose to modulate the forcing term in a way that depends on bubble size. We use an arctangent function because it is a continuously differentiable function, which does not produce discontinuities in the time derivatives. In addition, the cut-off position and steepness is easy to control.

The complete term for the neck-collapse function is given by

$$N(r_1, \theta, t) = \left(\frac{1}{2} - \frac{1}{\pi}\right) \tan^{-1}\{B(t - AR_1)\} \times \frac{9\kappa\sigma P_o \tan^2 \theta}{4\rho^2 R_1^5 \sin \theta} t^{469.5t+1.955}, \quad (4)$$

where  $A$  is a constant with the value of 1 and dimensions of  $\text{m}^{-1}\text{s}$ .  $B$  is a constant with the value 5000 and dimensions of  $t^{-1}$ .  $A$  and  $B$  were chosen arbitrarily so that a 2 mm bubble (on which Eq. (3) was based) has forcing which is almost unchanged, but a 0.5 mm bubble has forcing which only reaches a peak half as high as the 2 mm bubble. Figure 2 shows that the window function produces a reasonable but small variation in the forcing function with bubble size. The actual effect of these constants on the final acoustic signal is small because the dominant time period for driving the acoustic signal is the first few hundred microseconds, and this modulation has a limited effect during that period.

The second forcing term in Eq. (1) describes the effect of the pressure field radiated by bubble 2 on bubble 1, and vice versa. The acoustic pressure caused by the first bubble at 1 m distance is scaled to the pressure produced at the distance of the center of the second bubble, discussed below.

### C. Assumptions and limitations

The parameter  $D$  (the distance between the centers of the new bubbles) is estimated based on the angle  $\theta$ . For bubbles produced slowly at a nozzle, the ratio that is the distance from the conical tip to the rounded end of the bubble divided by the bubble diameter was observed to be 1.4. The measured angle  $\theta$  of the conical part of these bubbles is  $40^\circ$ . To

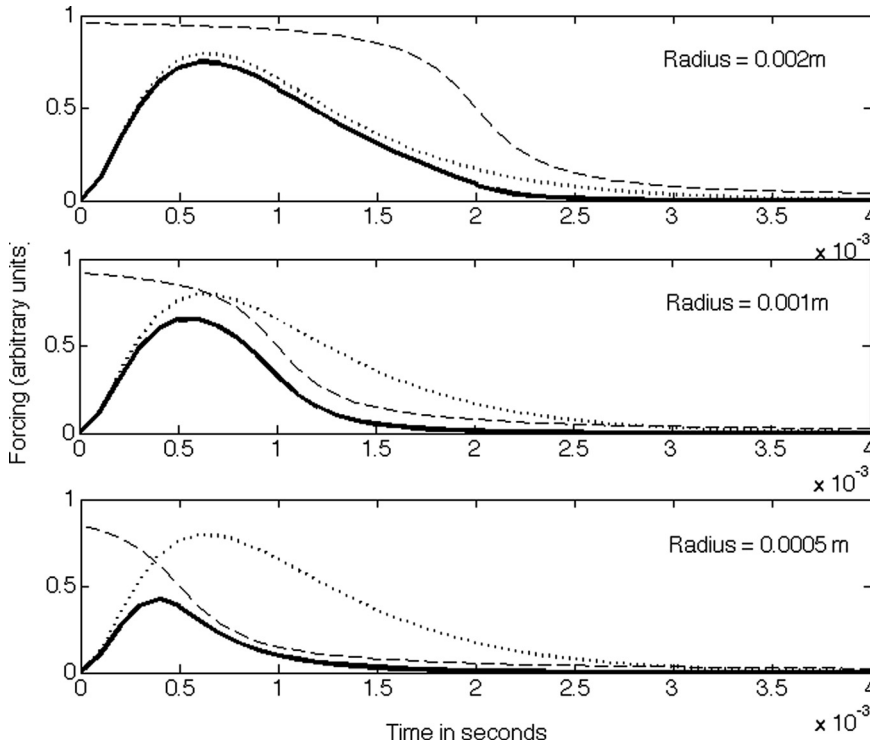


FIG. 2. The effect of the window on the driving force (see text for a full explanation). The dotted line in each case shows the forcing with time predicted by Eq. (3) for a 2 mm bubble. The dashed line shows the magnitude of the window term used to modulate the output of Eq. (3), and the heavy solid line shows the resulting forcing calculated from Eq. (4). The window used maintains the steep rise at the start (expected to be the same for all bubbles), but modulates the forcing with time after that.

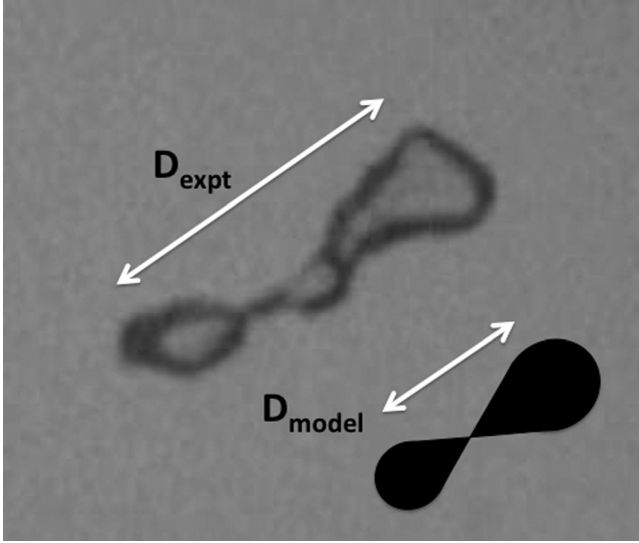


FIG. 3. A photograph of a real bubble close to the moment of pinch-off, compared with the silhouette of a two model bubbles with the same shape as bubbles from nozzles. In this and similar photographs, the complex shape of a real fragmenting bubble means that the actual bubble separation appears to be close to twice the separation of the simple model. This is the reason for the factor of 2 in Eq. (5).

estimate the distance  $D$  for other values of  $\theta$ , it was first assumed that the distance from the bubble center to the conical point was proportional to  $\cos \hat{\theta}$ . However, bubbles fragmenting in turbulence have very irregular shapes. Figure 3 shows a representative image taken during the experiment described in Deane and Stokes<sup>21</sup> with a silhouette to show an approximately equivalent event for bubbles shaped as if they were emerging from a nozzle. Examination of several similar images from that experiment suggests that the real bubble spacing is approximately twice that suggested by the simple nozzle model, so we use a value for  $D$  which is given by:

$$D = 2(R_1 + R_2)(1 + 1.04 \cos \theta). \quad (5)$$

This term is important because the acoustic pressure generated by a bubble falls off as  $1/R$ , and so the value used for  $D$  determines the magnitude of the pressure oscillation acting on the other bubble. Since the bubbles are so close together, the radiated pressure from the first bubble measured at the near and far sides of the second bubble will be significantly different. In this model, we assume that the pressure is uniform across the surface of the second bubble and that it can be represented as the pressure at the bubble centre, i.e., a distance  $D$  away from the first bubble.

For all the acoustic calculations, the bubbles are assumed spherical. Since the wavelength of the sound produced is so much larger than the bubble itself (the natural oscillation of a 2 mm radius bubble produces sound with a wavelength of approximately 0.9 m in water), we assume that the volume oscillation is the important process and that higher-order details of the shape of that volume are less significant. We take the shape into account in calculating the driving term produced by the bubble neck collapse, but assume a spherical bubble afterward. Longuet-Higgins<sup>27</sup> found that the additional volume due to the distortion of the

bubble when it has a conical neck can be neglected, so we make no distinction between the radius of curvature of the top half of the bubble at the point of pinch-off and the radius of the spherical bubble used for acoustic calculations.

We assume that the acoustic traces can be adequately fitted with a decaying sinusoid. This form will not match the trace well within the first period of oscillation when there is significant forcing but is a good approximation after that. In addition, this is the most practical fit to use when analyzing real data where the exact bubble shapes are unknown, so there is no point in refining the method for one type of idealized bubble here.

The neck angle is assumed to be the same for both bubbles, irrespective of the ratio of their radii. We justify this starting assumption with two points. The first is the observed behavior when a single bubble emerges from a nozzle. As the bubble grows, it is joined to the parent body of gas with a neck of air, and before detachment this neck narrows to a point. At the moment of pinch-off, the cone of air joined to the parent body of gas and the cone of air which is part of the bubble have very similar angles. This seems intuitive; as the neck radius decreases, the narrowest part of the neck will move along the neck toward the point where the surface tension parallel to the long axis of the bubble is approximately balanced. This balance can only occur if the neck angles are equal. The second point is that the original motivation for the neck-collapse model is the observed correlation between the energies of the two bubble fragments, suggesting symmetry in the dynamics driving the two bubbles into oscillation. Fragmentation in turbulence is a very dynamic event and it is unlikely that the bubble necks are conical with equal angles. However, it is a reasonable starting point for this model to estimate the magnitude of the driving force.

### III. MODEL PROCEDURE

The radius of the initial (parent) bubble was specified. The parameter  $L$  was chosen to include or exclude the non-linear terms, and the angle  $\theta$  for the neck was specified. A set of radius ratios  $r_1/r_2$  for the two new bubbles was defined and for each value of  $r_1/r_2$  the radii of the two daughter bubbles were calculated by conserving the volume of gas in the parent bubble. Then Eqs. (1) and (2) were integrated with time to get the surface displacement as the necks collapsed. The first simulation allowed the bubbles to interact with each other (the coupled case) and a separate, second simulation would allow them to respond to their own neck collapse only, ignoring the influence of the other bubble.

The acceleration of each bubble wall was then used to calculate the acoustic signal 1 m away from the pinch-off point for both coupled and uncoupled bubbles, and also the total acoustic signal due to each pair. These model results were then treated in the same way as experimental data would be, and they were analyzed by fitting decaying sinusoids to each computed acoustic signal. The general expression for a decaying sinusoid is given by

$$S_1 = A_1 \cos(\omega_1(t - t_1) + \phi_1) e^{(-\omega_1 \delta_1 t)/2}. \quad (6)$$

In general there are five parameters to be fitted: The amplitude  $A_1$ , frequency  $\omega_1$ , start time  $t_1$ , phase shift  $\phi_1$ , and

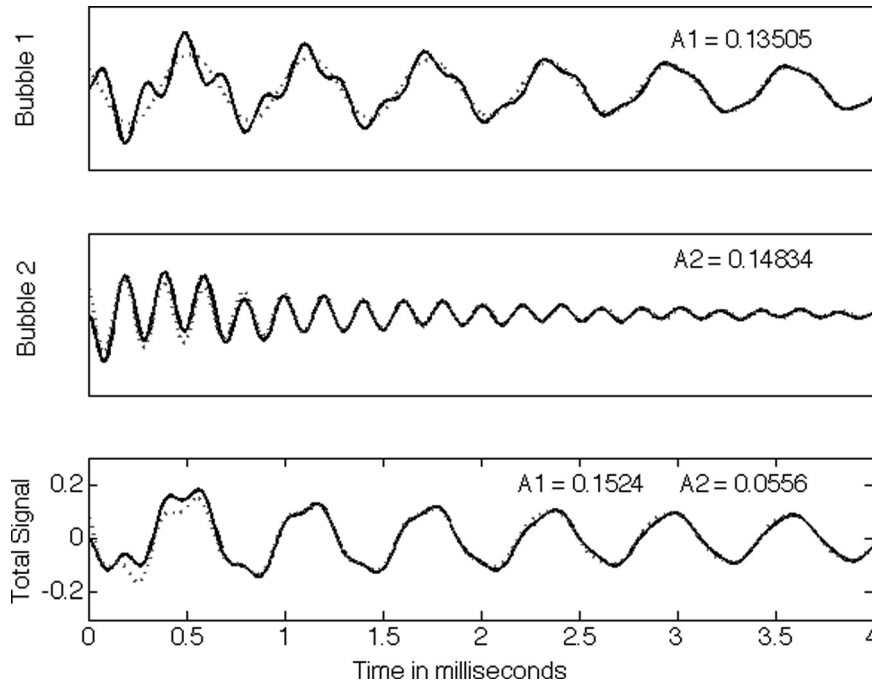


FIG. 4. Calculated acoustic signals for a 2 mm radius parent bubble with  $\theta = 40$  degrees and  $R_1/R_2 = 3$ . In each plot, the axes are the same. The bold line is the calculated acoustic output in Pascal at 1 m distance and the dotted line is the sinusoidal fit. The top two plots show the individual signal from the larger and smaller bubbles, respectively. The fitted amplitudes  $A_1$  and  $A_2$  are quoted on each plot. The third plot shows the eight-parameter fit to the combined signal, and the part cancellation of the higher frequency is evident in the fitted amplitude  $A_2$ .

dimensionless damping constant  $\delta_1$ . Because we use simulated data here, the start time is known and so we set  $t_1 = 0$ , which results in a four-parameter fit for one bubble and eight parameters for two bubbles [when we fit the sum of two decaying sinusoids of the form shown in Eq. (6)]. The eight-parameter fit from the simulations was then compared with the results of the experiment described in Deane and Stokes.<sup>21</sup>

The simplex search method was used to fit each acoustic trace and then the results were checked by eye. An example of a complete set of acoustic signals and the fits produced by each simulation is shown in Fig. 4. Signals for each bubble in both the coupled and uncoupled situations are fitted and a separate fit of the total coupled acoustic signal is also made.

Most of the simulations were carried out with a parent bubble radius of 2 mm, because this is approximately the size used in the experiments by Deane and Stokes, and we would like to make a direct comparison with those results. A few simulations were done with 1 mm radius bubbles to see whether non-linear effects were more important for these smaller bubbles.

The radius ratio  $r_1/r_2$  was limited to a maximum of 4. This is because of the uncertainty about both the neck-collapse function for the smaller bubble and the windowing increases as this ratio increases. These uncertainties arise because the forcing mechanism for small bubbles is not well-understood and consequently the simulation results for very small bubbles should be considered speculative. The radius ratio ranging from 1 to 4 is sufficient to make a comparison with the majority of the Deane and Stokes results.

The semi-angle of the conical neck is an important parameter. The analysis in Deane and Stokes<sup>21</sup> suggested that a range of semi-angles could account for the observed distribution of pressure pulse amplitudes, and a range of angles has been used in the calculations here. A bubble formed slowly at a nozzle has a neck angle of  $40^\circ$  and we ran the model for values of  $20^\circ$ ,  $30^\circ$ ,  $40^\circ$ ,  $50^\circ$ , and  $60^\circ$ . The surface tension used was always  $0.07 \text{ Nm}^{-1}$ .

#### IV. EXPERIMENTAL DATA

The data that we are using for comparison were initially presented and analyzed in Deane and Stokes.<sup>21</sup> The relevant features of the method will be summarized here for completeness, but for a full description the reader should consult the original publication.

Bubbles of approximately 2 mm radius were released from a nozzle at a rate of one every 2 s. As they rose through the water column, they passed through a region of turbulence caused by two opposing but offset jets. In many cases, this caused them to fragment into two or more daughter bubbles. A hydrophone placed 25 cm away recorded the acoustic emissions for subsequent analysis. The experiment was carried out at a depth of approximately 2 m in a large pool, which reduced the effects of reverberation to insignificant levels. Binary fragmentation events were fitted with two decaying sinusoids in a ten-parameter fit as described in Sec. III. These fitted parameters form the data set that we used to compare with the numerically simulated data generated for this study. The original acoustic signals were also available for comparison and are discussed in Sec. VI. The response of the hydrophone to a compression or rarefaction is an important element in the discussions which follow and this was carefully verified with the experimental hydrophones by both a squeeze test and discussion with the manufacturer.

#### V. COUPLING EFFECTS

In addition to our numerical simulations, we carried out a brief theoretical analysis to show the expected results for a system of coupled bubbles. With the exception of Fig. 5 (which shows the results of this section), all the results shown in this paper were calculated using the full damping terms show in Eqs. (1) and (2). However, in this section and since bubbles of this size have a high quality factor, we will ignore damping for the purposes of this simple calculation.

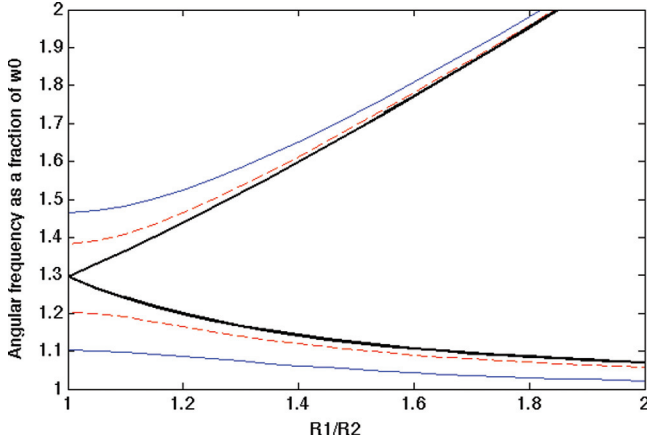


FIG. 5. (Color online) The calculated frequencies of the system of two daughter bubbles as a function of the bubble radius ratio. Thick solid lines indicate the frequencies in the uncoupled case, and the thin solid and dashed lines show the modified frequencies for a perfectly coupled system. This simple calculation ignores damping, but demonstrates the principle that a frequency gap is expected. Frequency is plotted relative to the natural frequency of the parent bubble,  $\omega_0$ . The thin solid lines represent bubbles with separation  $D$  (as shown in Fig. 1), which have a cone angle of  $40^\circ$ . The dashed lines represent bubbles with separation  $2D$ , to illustrate how the effect of coupling decreases as bubble separation increases.

We start with the coupled equations of motion for each bubble, which are simplified linear versions of Eqs. (1) and (2):

$$\begin{aligned} \frac{d^2 r_1}{dt^2} &= -\frac{3\kappa r_1 P_o}{\rho R_1^2} - \frac{R_2^3}{DR_1^2} \frac{d^2 r_2}{dt^2}, \\ \frac{d^2 r_2}{dt^2} &= -\frac{3\kappa r_2 P_o}{\rho R_2^2} - \frac{R_1^3}{DR_2^2} \frac{d^2 r_1}{dt^2}. \end{aligned} \quad (7)$$

These can be written in a coupled matrix form so that the eigenvalues  $\lambda$  of this equation will give the frequencies of the modes and the eigenvectors will give the relative amplitudes of the bubble displacements:

$$\begin{pmatrix} \alpha & \beta \\ \delta & \gamma \end{pmatrix} \begin{pmatrix} \varepsilon_1 \\ \varepsilon_2 \end{pmatrix} = \begin{pmatrix} \ddot{\varepsilon}_1 \\ \ddot{\varepsilon}_2 \end{pmatrix} = \lambda \begin{pmatrix} \varepsilon_1 \\ \varepsilon_2 \end{pmatrix} \quad \text{and} \quad \lambda = \omega^2. \quad (8)$$

Solving Eq. (8) allows us to calculate the expected oscillation modes for a system of two undamped coupled bubbles. The expected frequencies of this system of bubbles are shown in Fig. 5 as the ratio of bubble radii changes. As might be expected, coupled bubbles of similar size have eigenfrequencies significantly different from those of the uncoupled individual bubbles. The first mode corresponds to the two bubbles oscillating in phase and the second to antiphase oscillation.<sup>24</sup> A gap can be seen in Fig. 5 indicating that for a fixed size of parent bubble, there are some frequencies which cannot be produced by the daughter bubbles, even if they have sizes corresponding to those frequencies in a non-coupled situation. The addition of damping or a decrease in the coupling strength narrows the frequency gap. The existence of a suppressed range of frequencies is one of the most interesting consequences of accounting for bubble-bubble coupling, and it is also observed in the data, as shown in the Sec. VI.

It is important to note that while a bubble is a high- $Q$  oscillator, it can still be forced by nearby bubbles, especially

considering the close proximity of other daughter bubbles from the same parent bubble. Sound is scattered and re-radiated by the second bubble so that the acoustic pulse from each individual bubble can have multiple frequencies associated with it.

## VI. MODEL RESULTS

### A. Non-linearity

One of the aims of this research was to assess the effect of the non-linear terms in the Rayleigh-Plesset equation for fragmenting bubbles. Every simulation was run twice, once with and once without the non-linear terms. The difference that the non-linear terms make to the fitted amplitude is less than 2% for all radius ratios up to 4. This applies even under the most extreme conditions tested here: A parent bubble size of 1 mm and  $\theta = 60^\circ$ . These differences are not significant when the spread in the experimental data is considered. Only a small fraction of fragmentation events produce one bubble with a radius less than one quarter of the parent bubble radius and bubbles with radii less than 1 mm are expected to be stable against further fragmentation. We conclude that non-linear effects can be ignored in the interpretation of passive acoustic signals from bubbles fragmenting in turbulence within the range of bubble sizes investigated here.

### B. Antiphase mode

Figure 6 shows the fitted amplitude against frequency for both the simulated data and the real data, and although the frequency gap matches well, the high-frequency amplitudes do not. The discrepancy is associated with the antiphase mode, which always has the higher frequency. The energy from this mode is radiated in dipole form, so the contributions from each component of the system partially cancel each other out. The acoustic signals generated by the model were re-analyzed to investigate this. Table I shows

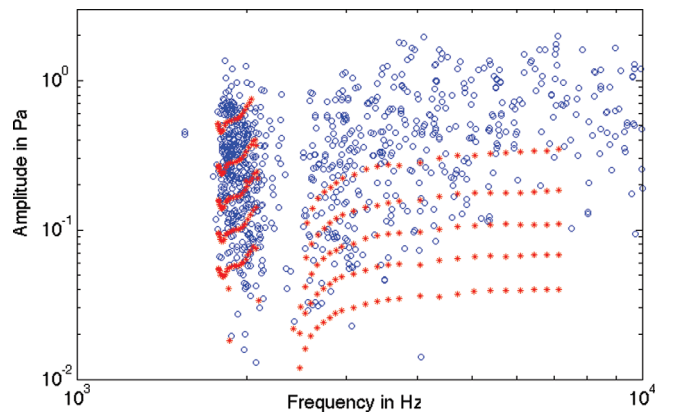


FIG. 6. (Color online) A comparison of the amplitude and frequency measured in an experiment and predicted by the model. Experimental data are shown by hollow symbols. Asterisks indicate the model results for different values of  $\theta$ . Larger values of  $\theta$  produce more energetic oscillations and the values used in the model are  $20^\circ$  (with the lowest amplitudes),  $30^\circ$ ,  $40^\circ$ ,  $50^\circ$ , and  $60^\circ$  (with the highest amplitudes). The frequency gap is a clear feature in both data sets, and the amplitudes of the larger bubbles are well-predicted by the model. As discussed in the text, the model underpredicts the amplitude of the smaller bubbles.

TABLE I. The individual modeled acoustic outputs from each daughter bubble can be analyzed separately, before they are added together to form the total acoustic output of the system. This table shows the results for  $R_1/R_2 = 1.3$ , so coupling is expected to be significant. A1 and F1 are the fitted amplitude and frequency of the lowest frequency fit, and A2 and F2 are the corresponding parameters for the higher-frequency fit. Parameters are shown for each bubble's acoustic signal individually and then for the fit to the total signal (which is the sum of the two components). In this case, the fitting algorithm could not find the high-frequency signal in the total signal, so an artifact was produced which is not shown here.

	A1	F1(Hz)	A2	F2(Hz)
Bubble 1	0.165	10 670	-0.06	15 784
Bubble 2	0.049	10 659	0.078	15 699
Total signal	0.183	10 704	—	—

the antiphase cancellation effect on the fitted parameters. Each individual bubble acoustic signal is fitted with two decaying sinusoids in an eight-parameter fit. It can be seen that once the two individual signals are added together and fitted again, the higher frequency is suppressed. In the case shown,  $R_1/R_2 = 1.3$  and the fitting algorithm fails to isolate the higher frequency. In these cases where there is only one dominant frequency, the fitting algorithm produces an artifact at a second very low frequency. These have been removed from the results shown in this paper. The dominance of the lower-frequency mode in this case suggests that it may not be possible to tell from the acoustic signal that binary fragmentation has occurred, since the oscillation seen is at one frequency only.

The reduced total amplitude of the antiphase mode is not observed in the experimental data, suggesting either that this mode starts with more energy than the in-phase mode, or that coupling effects are weak at the larger radius ratios. We discuss whether assumptions in the model could be responsible for this discrepancy in Sec. VI D below, but further work is required to explain this result.

### C. Energy correlation

The original motivation for the symmetrical neck-collapse model was that the large and small bubbles in a pair were observed to have highly correlated energies. Figure 7

shows two plots comparing the radiated acoustic energy of one bubble in a pair against the energy of the other bubble from the same pair. In both cases, the larger bubble is represented on the  $x$ -axis and the smaller bubble on the  $y$ -axis. The experimental data shows highly correlated energies. In the coupled model data there is a broad correlation over many orders of magnitude. However, the effect of the cancellation from the antiphase mode is evident, and the radiated energy at the lower frequency is almost always greater than the radiated energy at the higher frequency.

### D. General model discussion

The amplitude of modeled coupled bubbles as a function of frequency for various neck angles is shown in Fig. 6, along with experimental data. Both modeled and observed bubble systems show a similar suppressed frequency band at approximately 2.2 kHz. The distribution of the amplitudes at the lower frequencies is approximately reproduced by the range of semi-angles considered, although we have no direct evidence that different neck angles were responsible for this amplitude spread in the experimental data. However, the fact that varying this parameter reproduces the observed amplitude range suggests that the natural variation in bubble shapes as they fragment (and the consequences for the forcing mechanism) may account for the amplitude spread.

The amplitudes at the higher frequencies for the model data are almost an order of magnitude smaller than in the experimental data. This significant discrepancy between the predicted and observed amplitudes of the higher frequency radiation could be caused by either assumptions made about parameters in the model or the applicability of the model itself. There are several assumptions in the model, which could account for the discrepancy between the theoretical and experimental results. These are as follows:

- (1) Neglect of the difference between the incident pressure on the near and far side of each bubble. Geometrical spreading of the acoustic radiation will cause a difference.
- (2) The separation of the bubble centers was estimated by a simple model that was not based on experimental fragmentation results. This separation is the largest single factor controlling the coupling strength.

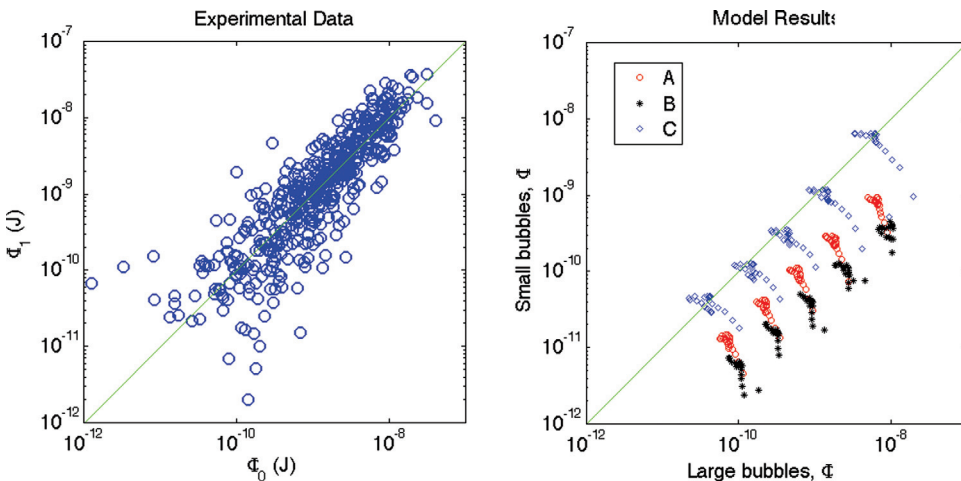


FIG. 7. (Color online) The panel on the left shows the experimental results for the total acoustic energy radiated at each frequency and is taken from Ref. 21, Fig. 8. The panel on the right shows the equivalent results from the models described in this paper. Series A is the basic model as described in Sec. II. Series B is a repeat of the simulation with the bubble separation arbitrarily halved. Series C shows model data with a single modification. The cone angle of the smaller bubble is  $20^\circ$  greater than the cone angle of the larger bubble, and this is an example of a small systematic change which will approximately produce equipartition of energy.



- (3) The bubbles are not spherical and this could affect coupling if the radiated acoustic signal is not the same in all directions in the near field.
- (4) We assumed that the bubble neck angles are equal in any single pair. The fact that the energies in a pair are correlated suggests that the neck angles are correlated (see Fig. 7), but this does not necessarily imply that they are equal.

We will now examine each of these assumptions to determine whether they can account for the discrepancy in small bubble amplitudes seen in Fig. 6.

### 1. Varying pressure across the bubble surface

The parameter  $D$  is used to approximate the separation of the bubble centers, and the forcing term assumes that the pressure at any given instant is the same everywhere on the surface of the bubble. However since the bubbles are separated by only a few radii, geometric spreading of the acoustic energy from the first bubble (assumed to radiate with spherical symmetry) will mean that the pressure on the near side of the second bubble is significantly higher than the pressure on the far side. This is ignored in the simulations described here because the Rayleigh-Plesset equations assume uniform pressure across the surface. We can do a simple calculation to estimate the effect of this assumption by integrating the pressure over the surface of the bubble while taking the geometric spreading into account. The bubble surface is considered to be made up of infinitesimally thin rings with the same axis as the bubble pair axis. The pressure at each distance is calculated assuming spherically diverging pressure from the first bubble, and we integrate  $PdA$  over the whole bubble surface. This can then be compared with the equivalent pressure at the bubble center multiplied by the bubble surface area, the quantity assumed in these calculations. In this simple calculation, these two quantities fortuitously turn out to be exactly equal, so we conclude that the method of using the fixed quantity  $D$  does not significantly affect the model results and is accurate to first order.

### 2. Bubble separation at the point of pinch-off

The coupled system has two oscillation modes, and the frequency gap between those two modes for equal-sized bubbles depends on the magnitude of the coupling. In this case, the extent of the interaction between the bubbles is almost entirely dependent on the bubble separation. We have assumed here that the separation of the bubble centers  $D$  is related to the neck angle, based on the shapes of bubbles emerging slowly from a nozzle. This leads to a typical estimate for  $D$  being approximately four times the sum of the bubble radii, given in Eq. (5). This value for  $D$  will have a large influence on the pressure coupling between the bubbles, since the radiated pressure decreases as  $1/R$ , and so we examine its influence on the results here. Figure 8 shows the effect of repeating the simulations shown in Fig. 6, but with the separation  $D$  arbitrarily changed by factors of 0.5, 0.75, 1, and 1.25. Reducing the coupling has two effects: The frequency gap narrows and the radiated pressure at the higher

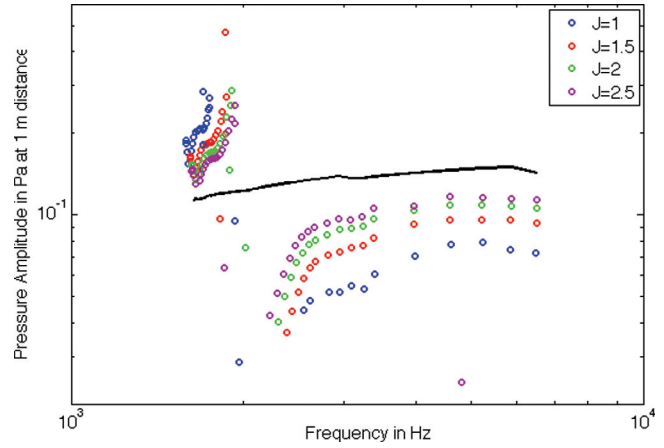


FIG. 8. (Color online) These are the model results for a 2 mm parent bubble and a cone angle of  $40^\circ$ . In each series, the distance separating the bubbles is the distance calculated using the different values of the prefactor  $J$  in Eq. (5). Most of the data shown in this paper were calculated with  $J = 2$ , and here we compare this with values of 1, 1.5, and 2.5. The central black line shows the expected amplitudes for uncoupled bubbles, for comparison. It can be seen that uncertainty in the bubble separation makes a considerable difference to the extent of the coupling. As  $J$  increases and the coupling strength decreases, the antiphase cancellation decreases and the frequency gap also decreases.

frequency increases significantly. Using the value of  $D$  as stated in Eq. (5) leads to a frequency gap which is well-matched with the gap in the data and also corresponds well with the photographic evidence. It is likely that the distance which separates the centers of the bubble volumes will vary from event to event, and Fig. 8 demonstrates that the tested range of bubble separations could lead to scatter in the measured high-frequency amplitude of about 15%. It seems that the distance  $D$  calculated in Eq. (5) is a reasonable estimate because the width of the frequency gap matches that in the data.

### 3. Non-spherical bubbles

Real bubbles fragmenting in turbulence are far from spherical. It is known that the acoustic pulse scattered from non-spherical bubbles is not spherically symmetrical.<sup>28</sup> In that study, elliptical bubbles only produced significantly non-spherical scattering when their aspect ratio was above 10. Bubbles fragmenting in turbulence can be highly distorted, but it seems unlikely that the aspect ratio would reach 10 without further fragmentation so this effect is discounted here. If it were significant during fragmentation events, it would decrease the effect of one bubble on the other slightly, since the bubbles in this study have a common long axis.

### 4. Equal neck angles

The symmetrical neck model was motivated by the high degree of correlation between the energy of each bubble in a pair. However, our results show that if the oscillatory energy for each bubble is approximately equal (a consequence of having equal neck angles) and the system is coupled, the radiated energies will not be equal. Figure 7 is a comparison of radiated energies at each of the two frequencies and shows the offset. Over many orders of magnitude there is still a strong correlation in energy, but the asymmetry is clear. The

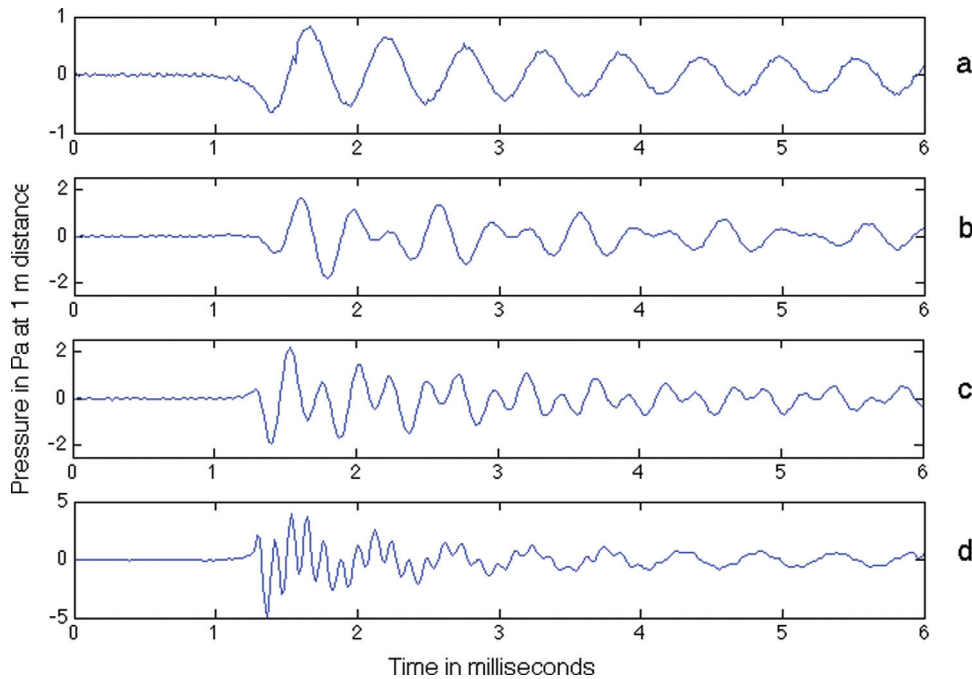


FIG. 9. (Color online) Four examples from the acoustic data collected in the experiment carried out by Deane and Stokes:<sup>21</sup> (a) A parent bubble emerging from the nozzle; (b) A binary fragmentation event which starts with a rarefaction, as (a) does, which can be explained by the neck-collapse model; (c) An intermediate case, where there is a small compression at the start of the acoustic signal; (d) The category of acoustic signal into which most of the measured events fall. The signal starts with a compression in the high-frequency component, although the lower-frequency component can be seen to start with a rarefaction similar to that in (a). This initial compression of the small bubble is not explained by the neck-collapse model outlined in this paper.

main assumptions affecting the coupling (detailed in the immediately preceding paragraphs) cannot explain this discrepancy. The effect of the small bubble on the larger bubble is to force oscillations in antiphase to the original oscillations, which cancel out a significant fraction of the total energy radiated at that frequency. This suggests that the smaller bubble may be systematically more energetic than this model predicts, compensating for the antiphase effect. There are two features of our model that could be altered to create this effect. One is the effect of the windowing process on the forcing. The other is the assumption of equal neck angles. For example, an approximate match to the real data is achieved if the neck angle of the smaller bubble is arbitrarily chosen to be  $20^\circ$  greater than the neck angle of the larger bubble. Figure 7 illustrates this. We are not suggesting that the neck angle of the smaller bubble actually is necessarily  $20^\circ$  higher, but we are simply pointing out that a relatively modest increase in neck angle is sufficient to account the equipartition of energy between the oscillatory modes.

## VII. COMPARISON OF MODEL RESULTS AND DATA

An important feature of all the total acoustic signals generated in this study is that they always start with a rarefaction, and this is also the case for a single bubble released from a nozzle.<sup>20</sup> The acoustic signal generated by the larger bubble of the pair will have a higher-frequency component generated by coupling with the smaller bubble, and this may mean that this larger bubble alone does emit a signal starting with a compression. However, the hydrophone can only record the sum of both signals and energy conservation makes it impossible for this initial high-frequency compression of the larger bubble to radiate with a greater amplitude than the emitted rarefaction from the smaller bubble. This means that a direct consequence of having a driving mechanism caused by an initial volume decrease in both bubbles is that the overall pair

acoustic signal must begin with a rarefaction. However, examination of the acoustic signals recorded shows that many binary fragmentation signals begin with a compression.

The binary fragmentation signals can be organized into three groups by their shape in the first millisecond. The first group starts with a rarefaction, which is the same as a single bubble released from a nozzle. The second group is a borderline group, having either a very small compression or a very small rarefaction before the first large oscillation. Members of the third group start with a significant compression. Representative examples of each case are shown in Fig. 9 and the acoustic signal produced by a single bubble at a nozzle is shown at the top for comparison. In the data set shown here, there are 194 cases where the acoustic signal starts with a clear compression and 58 start with a clear rarefaction. Forty-eight cases fall into the middle category. In every case, the compression was in the high-frequency component, and the lower-frequency component always started with a rarefaction. This suggests that the neck-collapse model applies consistently for the larger bubble of the pair, but only approximately a quarter of the time for the smaller bubble.

Figure 10 shows the same frequency and amplitude data as Fig. 6, but different symbols are used for signals with an initial compression and an initial rarefaction. It can be seen that the initial rarefaction occurs in the majority of cases where the radius ratio is between 1 and 2, and rarely at larger radius ratios, and so there is a size dependence. Although the mechanism appears to be related to bubble size, the oscillation energy does not appear to depend on the mechanism. As stated earlier, there is no means whereby the current model for the neck-collapse process can account for a wave with an initial compression. This suggests that the double-neck collapse model investigated here is appropriate for fragmentation events that produce large or equally sized bubbles, but a modification is required to understand the other cases. The discussion of coupling effects in this paper is still valid,

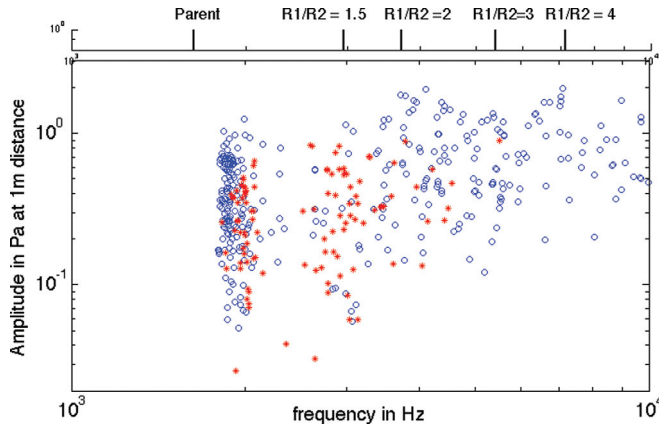


FIG. 10. (Color online) These are the data shown in Fig. 6, but the circles represent events where the acoustic signal began with a compression, and the asterisks indicate events where the acoustic signal began with a rarefaction. It can be seen that rarefaction events are most likely when the two new bubbles are very similar in size, and that these events do not produce the highest amplitudes.

since the driving mechanism only affects the amplitude and not the frequency of oscillation or the coupling behavior. We will not speculate on the mechanism driving these small bubbles, other than to note that it must be associated with a rapid volume increase on pinch-off, in order to generate the initial compression observed.

## VII. DISCUSSION

The effect of coupling on frequency (and therefore on the interpretation of bubble size) is only significant for similarly sized pairs of bubbles. Understanding of the gap in the frequency histogram in Fig. 6 is clearly important for interpreting the acoustics of bubbles that start with a known size and then fragment. However, in a population of naturally occurring bubbles (where the parent bubbles have a range of sizes), the size of the parent bubble is not known. An important question to address is whether knowledge of the effects of coupling would have a significant effect on the interpretation of acoustic data arising from such a situation. Its importance will depend on the likelihood of different fragmentation ratios. If the probability of an equal volume split is high, the effect of coupling would be more significant, whereas if those events are rare, the effects of coupling on interpretation would be negligible.

Interpretation of passive acoustic signals from fragmentation could be affected by coupling in two main ways. The mixture of the in-phase and antiphase modes for bubbles of roughly equal size depends on the initial boundary conditions, which will be altered if the two new bubbles have different timescales of neck collapse. If the dominant mode is the in-phase one, the acoustic signal may resemble that of a single excited large bubble instead of two similarly sized smaller ones. If the dominant mode is the antiphase mode, the acoustic radiation from the two bubbles may largely cancel out. This would reduce the likelihood of detection, and it may explain our observation that fragmentation events resulting in two similarly sized bubbles tend to be quiet. Either way, the bubble population would be underestimated. These effects are mostly likely to matter when the bubbles are similarly sized

(with a radius ratio between one and two) and it might be possible to correct for them if the fragmentation probability density function was better known. The case of the in-phase mode dominating to produce a single frequency signal is distinguishable from a single excited bubble because the damping is different (it is greater by a factor of approximately 2). However, the cases when the antiphase mode dominates so that the event is very quiet are harder to correct for. Laboratory observation might provide an indication of the relative likelihood of these two events, allowing for a correction.

Bubble coupling and the existence of the in-phase mode could account for the “type A2” bubbles observed by Medwin and Beaky.<sup>29</sup> These were identified as those which produce an acoustic signal similar to that of a single spherical bubble, but with an initial damping almost twice as great as the theoretical damping. We noticed that this may be explained by a comparison of the acoustic signal from a single new bubble with radius  $R$  (for example, a new bubble formed at a nozzle), and the acoustic signal produced by a bubble of radius  $R$  fragmenting into two equally sized new bubbles. Our coupled model predicts that for equally sized daughter bubbles, the damping of the lower-frequency signal is approximately twice that expected for the single bubble with the radius of the parent bubble. The higher-frequency component is almost completely cancelled out, so the acoustic signal from the fragmenting bubble appears to be that of a single bubble with twice the expected damping, as they describe. The overall effect would be to allow the sound pulse from a binary fragmentation event to be inadvertently identified as coming from a single larger bubble, but with an anomalous damping.

### A. Model applicability

One of the most obvious effects of coupling is that new bubble pairs with equal energy partition radiating more energy at the lower frequency than the higher one. The energies inferred from analysis of the modeled coupled bubble acoustic pulses are strongly correlated, but not equal, whereas an uncoupled analysis of the experimental data implies equal energy partition. The explanation for the discrepancy is likely to be one of three issues. The first is that the assumptions made in the simplified model used here are inadequate, and that the real distorted bubble shapes and surrounding flow field have a strong influence on the acoustic output. The second is that the neck-collapse model is not appropriate for smaller bubbles, either because some other mechanism is driving the smaller bubble or that our assumptions for how the neck forcing changes as bubble size decreases are inadequate. The third is that the simplified description of bubble interaction presented here does not apply for bubbles of very different sizes. That is, a fragmentation pair composed of a very large and a very small bubble may not behave as a coupled system. Further work is required to understand why the smaller bubble is more energetic than our simple neck-collapse model would predict.

## VIII. CONCLUSIONS

It was recently found that the sound emitted by a newly formed single bubble is consistent with the volume forcing

caused by the rapidly collapsing neck of air accompanying formation. In the research described here, this neck-collapse model was extended to simulate one bubble fragmenting into two coupled bubbles, and the resulting calculated acoustic signals were compared with experimental data. The acoustic coupling of the two new bubbles had a significant effect on the amplitude and frequency of the emitted acoustic pulse, especially when the ratio of the radii of the two new bubbles was between 1 and 2. For any given parent bubble size, coupling causes a gap in the frequencies that can be produced because the two new bubbles form a single oscillatory system with an in-phase mode and an antiphase mode. The initial conditions at the moment of fragmentation determine which mode dominates. The frequency gap is seen in both the theoretical results and the experimental data of Deane and Stokes.<sup>21</sup> Dominance of the in-phase mode of equal-sized bubble products from a fragmentation event can also explain Medwin and Daniels' observation of A2 type bubble pulses.

The lower-frequency part of the acoustic signal always starts with a rarefaction, both in the model results and the experimental data. This is consistent with the larger bubble always being driven by neck collapse. The neck-collapse model also predicts the range of amplitudes seen in the experimental data for the larger bubble. One quarter of the acoustic signals observed imply that the small bubble signal started with a rarefaction and so the double-neck collapse model can account for these. However, in the remaining fragmentation events the small bubble oscillation started with a compression, implying a different or modified driving mechanism. For example, the jet of water generated by the collapsing neck may play a dominant role in the excitation of small bubble products.

The comparison of experimental data and model results demonstrates that acoustic coupling is important for bubble fragmentation products of approximately equal size. We expect that knowledge of these coupling effects will improve the interpretation of passive acoustic data from bubbles fragmenting in turbulence.

## ACKNOWLEDGMENTS

We would like to thank Dale Stokes and James Uyloan for help with the experimental data collection. We gratefully acknowledge financial support from the Office of Naval Research (Grant No. N00014-04-1-072828) and the National Science Foundation (Grant No. OCE 07-27140).

<sup>1</sup>D. M. Farmer, C. L. McNeil, and B. D. Johnson, "Evidence for the importance of bubbles in increasing air-sea gas flux," *Nature* **361**, 620–623 (1993).

<sup>2</sup>R. F. Keeling, "On the role of large bubbles in air-sea gas exchange and supersaturation in the ocean," *J. Mar. Res.* **51**, 237–271 (1993).

- <sup>3</sup>R. Hamme and S. Emerson, "Mechanisms controlling the global oceanic distribution of the inert gases argon, nitrogen and neon," *Geophys. Res. Lett.* **29**, 35-1–35-4 (2002).
- <sup>4</sup>G. Deane and M. D. Stokes, "Scale dependence of bubble creation mechanisms in breaking waves," *Nature* **418**, 839–844 (2002).
- <sup>5</sup>D. M. Farmer, S. Vagle, and A. D. Booth, "A free-flooding acoustical resonator for measurement of bubble size distributions," *J. Atmos. Ocean. Technol.* **15**, 1132–1146 (1998).
- <sup>6</sup>T. Leighton, S. Meers, and P. White, "Propagation through nonlinear time-dependent bubble clouds and the estimation of bubble populations from measured acoustic characteristics," *Proc. R. Soc. A* **460**, 2521–2550 (2004).
- <sup>7</sup>H. Medwin and A. C. Daniel, "Acoustical measurements of bubble production by spilling breakers," *J. Acoust. Soc. Am.* **88**, 408–412 (1990).
- <sup>8</sup>T. G. Leighton and A. J. Walton, "An experimental study of the sound emitted from gas bubbles in a liquid," *Eur. J. Phys.* **8**, 98–104 (1987).
- <sup>9</sup>M. R. Loewen and W. K. Melville, "A model of the sound generated by breaking waves," *J. Acoust. Soc. Am.* **90**, 2075–2080 (1991).
- <sup>10</sup>R. Manasseh, R. F. LaFontaine, J. Davy, I. Shepherd, and Y.-G. Zhu, "Passive acoustic bubble sizing in sparged systems," *Exp. Fluids* **30**, 672–682 (2001).
- <sup>11</sup>G. Deane and M. D. Stokes, "The acoustic signature of bubbles fragmenting in sheared flow," *J. Acoust. Soc. Am.* **120**, EL84 (2006).
- <sup>12</sup>A. Prosperetti, "Thermal effects and damping mechanisms in the forced radial oscillations of gas bubbles in liquids," *J. Acoust. Soc. Am.* **61**, 17–27 (1977).
- <sup>13</sup>T. G. Leighton, *The Acoustic Bubble* (Academic, London, 1994), p. 155.
- <sup>14</sup>M. S. Plesset and A. Prosperetti, "Bubble dynamics and cavitation," *Annu. Rev. Fluid Mech.* **9**, 145–185 (1977).
- <sup>15</sup>H. C. Pumphrey, J. E. Ffowcs-Williams, "Bubbles as sources of ambient noise," *IEEE J. Ocean. Eng.* **15**, 539–567 (1990).
- <sup>16</sup>M. S. Longuet-Higgins, "An analytic model of sound production by raindrops," *J. Fluid Mech.* **214**, 395–410 (1990).
- <sup>17</sup>R. D. Hollet and R. M. Heitmeyer, "Noise generation by bubbles formed in breaking waves," in *Sea Surface Sound* (Kluwer, Boston, 1998), pp. 449–462.
- <sup>18</sup>R. Manasseh, S. Yoshida, and M. Rudman, "Bubble formation processes and bubble acoustic signals," in *Proceedings of the Third International Conference on Multiphase Flow (ICMF'98)*, Lyon, France (June 8–12, 1998), paper no. 202.
- <sup>19</sup>R. Manasseh, A. Bui, J. Sandercock, and A. Ooi, "Sound emission processes on bubble detachment," in *Proceedings of the 14th Australasian Fluid Mechanics Conference*, Adelaide, South Australia (December 9–14, 2001), edited by Dally, Vol. 1, pp. 857–860.
- <sup>20</sup>G. B. Deane and H. Czerski, "A mechanism stimulating sound production from air bubbles released from a nozzle," *J. Acoust. Soc. Am.* **123**, EL126 (2008).
- <sup>21</sup>G. B. Deane and M. D. Stokes, "The acoustic excitation of air bubbles fragmenting in sheared flow," *J. Acoust. Soc. Am.* **124**, 3450–3463 (2008).
- <sup>22</sup>M. Ida, "A characteristic frequency of two mutually interacting gas bubbles in an acoustic field," *Phys. Lett. A* **297**, 210–217 (2002).
- <sup>23</sup>P. Hsiao, M. Devaud, and J. Bacri, "Acoustic coupling between two air bubbles in water," *Eur. Phys. J. E* **4**, 5–10 (2001).
- <sup>24</sup>V. Leroy, M. Devaud, and J. Bacri, "The air bubble: Experiments on an unusual harmonic oscillator," *Am. J. Phys.* **70**, 1012–1019 (2002).
- <sup>25</sup>H. Medwin, *Sounds in the Sea* (Cambridge University Press, 2005), equation 6.72b, p. 187.
- <sup>26</sup>A. Prosperetti, L. Crum, K. Commander, "Non-linear bubble dynamics," *J. Acoust. Soc. Am.* **83**, 502–514 (1988).
- <sup>27</sup>M. Longuet-Higgins, "The release of air bubbles from an underwater nozzle," *J. Fluid Mech.* **230**, 365–390 (1991).
- <sup>28</sup>C. Feuillade and M. F. Werby, "Resonances of deformed gas bubbles in liquids," *J. Acoust. Soc. Am.* **96**, 3684–3692 (1994).
- <sup>29</sup>H. Medwin and M. M. Beaky, "Bubble sources of the Knudsen sea noise spectra," *J. Acoust. Soc. Am.* **86**, 1124–1130 (1989).